

## Conductivity in percolation networks with broad distributions of resistances

J. Machta, R. A. Guyer, and S. M. Moore\*

*Department of Physics and Astronomy, University of Massachusetts, Amherst, Massachusetts 01003*

(Received 11 November 1985)

Diluted resistor networks with a broad distribution of resistances are studied near the percolation threshold. A hierarchical model of the backbone of the percolation cluster is employed. Resistor networks are considered where the resistors,  $R$ , are chosen from a distribution having a power-law tail such that  $\text{Prob}\{R > X\} \sim X^{-\alpha}$  as  $X \rightarrow \infty$ ,  $0 < \alpha < 1$ . Such distributions arise naturally in continuum percolation systems. The hierarchical model is studied numerically and using a renormalization-group transformation for the distribution of resistances. The conclusion is that the conductivity exponent  $t$  is the greater of  $t_0$  and  $(d-2)\nu + 1/\alpha$  where  $t_0$  is the universal value of the conductivity exponent and  $\nu$  is the correlation-length exponent. This result is in agreement with Straley's earlier predictions [J. Phys. C 15, 2333 (1982); 15, 2343 (1982)].

### I. INTRODUCTION

In this paper we study the conductivity near percolation of diluted resistor networks with a broad distribution of resistances. We consider bond percolation with a fraction,  $p$ , of finite resistors chosen from a distribution having a power-law tail such that

$$\text{Prob}\{R > X\} \sim X^{-\alpha} \quad \text{as } X \rightarrow \infty. \quad (1.1)$$

Here  $R$  is any of the finite resistors of the network and  $0 < \alpha < 1$  characterizes the tail of the distribution. An important feature of such distributions is that they have no mean value. Our object is to understand the conductivity exponent,  $t$ , which characterizes the singularity of the conductivity,  $\sigma \sim (p - p_c)^t$ .

It has recently been shown that a number of continuous random systems with percolation thresholds have transport properties near the threshold which are influenced by a broad distribution of bond strengths. A class of models of random materials which displays this phenomenon are the Swiss-cheese models<sup>1,2</sup> in which randomly placed, spherical holes perforate a conducting or elastic medium. A related model which is important in the foundations of nonequilibrium statistical mechanics is the overlapping Lorentz gas<sup>3,4</sup> in which a single particle moves classically in an array of overlapping hard spherical scatterers. These models have been analyzed<sup>1,4</sup> by mapping the continuum system onto a random network with a distribution of resistances (elasticities for elastic Swiss-cheese or waiting times for the Lorentz gas) satisfying (1.1) where  $\alpha$  depends on the dimensionality and type of transport in each case, large resistances arise when three spheres ( $d$  hyperspheres) are arranged so that only a small conducting neck is left between them.

On a more fundamental level, understanding the effect of a distribution of resistances on the conductivity exponent clarifies the scope of the universality hypothesis and leads to interesting insights into the relation between the renormalization-group approach and the theory of stable distributions.

The problem of percolation in the presence of a broad

distribution of bond strengths was first studied by Kogut and Straley<sup>5</sup> and later by Ben-Mizrahi and Bergman,<sup>6</sup> Straley,<sup>7</sup> Halperin *et al.*,<sup>1</sup> Sen *et al.*,<sup>8</sup> and Tremblay and Lubensky.<sup>9</sup> These investigations all arrive at the conclusion that an anomalous distribution with a sufficiently small value of  $\alpha$  (Ref. 10) leads to nonuniversal values of  $t$ , but they disagree in their detailed predictions. In this paper we take a new approach to the problem which is in agreement with Ref. 7 and clarifies some of the arguments presented there.

In Ref. 7 Straley reaches the conclusion that the observed exponent  $t$  is the greater of the universal value  $t_0$  and a quantity  $t(\alpha)$  given below. His argument is based upon a numerical study of the evolution of the probability distribution of the resistors under a simple real-space renormalization-group transformation. He finds that the large- $R$  tail of the distribution evolves independently of the rest of the distribution and dominates the fixed point when  $\alpha$  is sufficiently small, leading to the result  $t = t(\alpha)$ . For larger  $\alpha$ , the tail becomes unimportant at the fixed point and  $t = t_0$ . He asserts that the crossover between  $t_0$  and  $t(\alpha)$  occurs when the two are equal. In order to obtain  $t(\alpha)$  he uses the nodes-links<sup>11</sup> picture of the backbone of the percolation cluster and ignores multiply-connected insertions between nodes or blobs, arguing that the distribution of blob resistances can be ignored. Thus he considers the percolation backbone to be a network of nodes separated by the correlation length  $\xi$  and connected by chains of random resistors in series. The final step in his argument is the application of Coniglio's<sup>12</sup> result that the number of singly connected bonds or links in a chain,  $S$ , diverges according to  $S \sim (p - p_c)^{-1}$ . Since the typical value of the sum of  $S$  independent random variables chosen from a distribution satisfying (1.1) diverges as  $S^{1/\alpha}$  for  $0 < \alpha < 1$ , he obtains the result

$$t(\alpha) = (d-2)\nu + 1/\alpha, \quad (1.2)$$

where  $d$  is the dimension of the system and  $\nu$  is the correlation-length exponent. The term proportional to  $\nu$  relates the conductances to the conductivity of the lattice.

While presenting a convincing intuitive picture of the

behavior of  $t$ , Straley's analysis raises some questions. Can the crossover between  $t_o$  and  $t(\alpha)$  be derived from an analytical theory? Is it correct that the blobs in the more accurate nodes-links-blobs<sup>13</sup> description of the backbone do not contribute to  $t(\alpha)$ ? In the present work we address these questions in the context of a recently proposed<sup>14</sup> hierarchical model of the percolation backbone. In Sec. II the model is defined and studied analytically using an exact renormalization-group method. In Sec. III the model is studied numerically, confirming the validity of the analytic results found in Sec. II and illustrating the evolution of the probability distribution of the resistances under renormalization. The paper closes with a discussion.

## II. THE HIERARCHICAL MODEL AND AN ANALYTIC STUDY OF THE CONDUCTIVITY EXPONENT

In this section we introduce a class of hierarchical models for the backbone of the infinite cluster. Using this class of models we give an argument for the scaling properties of the conductivity of the infinite cluster when the resistors are anomalously distributed, (1.1).

### A. The hierarchical model

In the nodes-links-blobs picture<sup>13</sup> the backbone of the infinite cluster is taken to be a disordered  $d$ -dimensional lattice with typical spacing  $\xi$ , where  $\xi$  is the correlation length. The sites of this lattice are referred to as nodes and the bonds as chains. The chains are composed of singly-connected pieces or links and multiply-connected pieces or blobs. The blobs are arranged in a hierarchical fashion in that, when the chain is viewed on longer length scales, some of the smaller blobs of a given size are seen to be incorporated into larger blobs.<sup>15</sup> We introduce a hierarchical model of a chain described by three parameters,  $a$ ,  $b$ , and  $c$ . The model is defined by a set of rules for assembling an  $(n+1)$ th generation chain, or  $(n+1)$ -chain, from  $n$ -chains. These rules are the following:

(1) The length of an  $(n+1)$ -chain,  $L^{(n+1)}$ , is a factor  $b$  greater than the length of an  $n$ -chain,  $L^{(n)}$ ,

$$L^{(n+1)} = bL^{(n)}. \quad (2.1a)$$

(2) An  $(n+1)$ -blob is a multiply-connected network of  $n$ -chains constructed in the same way at each generation so that, if the resistance of each  $n$ -chain is  $R^{(n)}$ , then the resistance of the  $(n+1)$ -blob,  $R_{\text{blob}}^{(n+1)}$ , is given by

$$R_{\text{blob}}^{(n+1)} = aR^{(n)}. \quad (2.1b)$$

(3) An  $(n+1)$ -chain is composed of  $c$   $n$ -chains connected in series with one  $(n+1)$ -blob. Thus, if each  $n$ -chain has resistance  $R^{(n)}$ , the resistance of the  $(n+1)$ -chain is given by

$$R^{(n+1)} = cR^{(n)} + R_{\text{blob}}^{(n+1)}. \quad (2.1c)$$

Note that  $c$  also specifies the way in which the number of links in an  $n$ -chain,  $S^{(n)}$ , scales,

$$S^{(n+1)} = cS^{(n)}. \quad (2.2)$$

Thus, using the result  $S \sim (p - p_c)^{-1}$ , we have

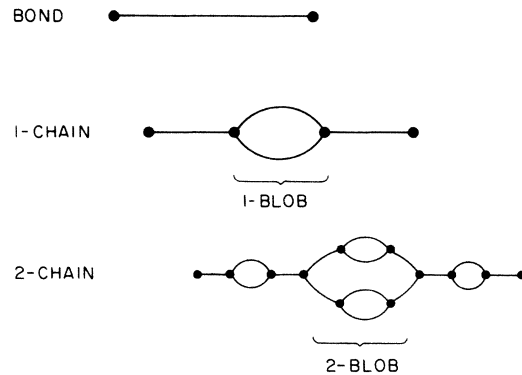


FIG. 1. Construction of the hierarchical lattice used in the simulation. An  $(n+1)$ -generation blob is formed from two parallel  $n$ -generation chains. An  $(n+1)$ -chain is composed of an  $(n+1)$ -blob in series with two  $n$ -chains. The first two generations of the construction are illustrated.

$$\nu = \ln b / \ln c. \quad (2.3)$$

These considerations are illustrated in Fig. 1. The hierarchical construction specified by these rules continues until the length of the chain reaches the correlation length. The backbone is then constructed as a regular lattice of chains of length  $\xi$ .

In this section we shall not need to precisely specify the geometrical way in which an  $(n+1)$ -blob is constructed from  $n$ -chains. In the next section we numerically study a hierarchical model in which  $c=2$ ,  $b=3$ , and the  $(n+1)$ -blob is formed from two parallel  $n$ -chains so that  $a = \frac{1}{2}$ . This is the  $d=2$  version of the models discussed by de Arcangelis *et al.*,<sup>14</sup> where, for  $1 \leq d \leq 6$ , they let  $c = 8/(6-d)$ ,  $b = c + 1$ , and construct the blobs from two parallel chains. With this model they find good agreement with known values of percolation exponents.

### B. The conductivity exponent

For ordinary percolation with each bond having the same resistance,  $R^{(0)}$ , and length,  $L^{(0)}$ , the conductivity exponent can be related to  $a$ ,  $b$ , and  $c$  by a simple argument. At each generation the resistance  $R^{(n)}$  of an  $n$ -chain is given by

$$R^{(n)} = (c+a)^n R^{(0)}, \quad (2.4)$$

while the length of an  $n$ -chain is given by

$$L^{(n)} = b^n L^{(0)}. \quad (2.5)$$

Let  $l$  be the number of generations required to reach the correlation length; then  $\xi = L^{(l)}$  and the conductivity  $\sigma$  is given by

$$\sigma = \xi^{(2-d)} / (c+a)^l R^{(0)}. \quad (2.6)$$

Thus the conductivity exponent  $t$  (defined by  $\sigma \sim \xi^{-t/\nu}$ ) is

$$t_o / \nu = (d-2) + \ln(c+a) / \ln b, \quad (2.7)$$

where the subscript  $o$  refers to ordinary percolation as opposed to percolation where randomness in the resistors is relevant.

Next let us turn to the situation where the resistors forming the backbone are chosen from a probability distribution satisfying (1.1). In this case the resistance of an  $n$ -chain is a random variable. Thus the scaling law,  $R^{(n)} = (c+a)^n R^{(0)}$ , is incorrect and we must consider the probability distributions for  $n$ -chains and  $n$ -blobs. The correct relation between the random variables is

$$R^{(n+1)} = R_{\text{blob}}^{(n+1)} + \sum_{j=1}^c R_j^{(n)}, \quad (2.8)$$

where  $R_j^{(n)}$  are the resistances of  $c$   $n$ -chains chosen independently from the  $n$ -chain probability distribution. In general,  $R_{\text{blob}}^{(n+1)}$  is a nonlinear function of a finite number of independently chosen  $n$ -chain resistances. For example, if the blobs are formed from two parallel chains we would have

$$R_{\text{blob}}^{(n+1)} = (1/R_1^{(n)} + 1/R_2^{(n)})^{-1}. \quad (2.9)$$

The evolution of a probability distribution under a nonlinear transformation such as (2.8) and (2.9) is difficult to study analytically. To render the problem tractable, we make the following approximation. We assume that the resistance of each  $(n+1)$ -blob is given by the definite value,

$$R_{\text{blob}}^{(n+1)} = ar^{(n)}, \quad (2.10)$$

where  $r^{(n)}$  is a typical value of the resistance of the  $n$ -chains, to be defined below, and  $a$  is defined in (2.1b). The justification for this approximation is that the distribution of the blob resistances is much narrower than the distribution of the chain resistances forming the blob. This is because the parallel paths within a blob allow current to bypass the largest resistors. For example, consider the case that blobs are constructed from  $k$  parallel chains. If  $\alpha$  describes the tail of the distribution of chain resistances [see (1.1)], then it is easy to show that  $k\alpha$  describes the tail of the distribution of the resulting blob resistances. Thus the blobs are distributed in a less singular way than the chains from which they are composed.

Given this approximation it is possible to analyze the evolution of the chain probability distribution using Laplace transform techniques.<sup>16</sup> For a cumulative probability distribution  $F(x)$  which vanishes for  $x < 0$ , we define the Laplace transform  $f(z)$  as

$$f(z) = \int \exp(-zx) dF(x), \quad (2.11)$$

and its natural logarithm  $g(z)$ ,

$$g(z) = -\ln f(z). \quad (2.12)$$

For a random variable  $R$  with the definite value  $r_0$ ,  $g_R(z) = zr_0$ . For a random variable  $R$  which satisfies (1.1) a Tauberian theorem shows that  $g_R(z) \sim z^\alpha$  as  $z \rightarrow 0$ . Finally, if a random variable  $R$  is a sum of random variables,  $R = R_1 + R_2 + \dots + R_k$ , then the associated probability density for  $R$  is a convolution of the densities for  $R_1, R_2, \dots, R_k$  and, by the convolution theorem for Laplace transforms,  $g_R = g_{R_1} + g_{R_2} + \dots + g_{R_k}$ .

The convolution theorem for Laplace transforms shows that the  $g$ 's associated with these random variables enjoy the same linear relation as the variables themselves. Thus,

using (2.8) and (2.10) we have a recursion relation for the functions  $g^{(n)}$  corresponding to the probability distributions for the  $n$ -chain resistances:

$$g^{(n+1)}(z) = ar^{(n)}z + cg^{(n)}(z). \quad (2.13)$$

This recursion relation is closed by defining the typical value. We choose the following definition for the typical  $n$ -chain resistance  $r^{(n)}$ ,

$$g^{(n)}(1/r^{(n)}) = 1. \quad (2.14)$$

This definition has several convenient properties. Firstly, it is well defined even for distributions which have no mean value. Secondly, if two random variables are related by a scale change, then their corresponding typical values are related by the same scale change. Finally, for narrow distributions, the typical value is close to the mean. These properties of the typical value are discussed in more detail in the Appendix.

Our object is to determine the scaling behavior of the  $n$ -chain probability distributions characterized by  $g^{(n)}$ . This is most easily accomplished by constructing a renormalization-group (RG) transformation in which the distribution is rescaled by a factor  $\lambda$  at each iteration so that the typical value is always equal unity. The RG transformation of  $g$  obtained from (2.13) is

$$g^{(n+1)}(\lambda^{(n+1)}z) = az + cg^{(n)}(z), \quad (2.15)$$

and, from (2.14),  $\lambda^{(n)}$  is chosen so that

$$g^{(n)}(z=1) = 1. \quad (2.16)$$

We seek to find the fixed points of this transformation within a suitably large space of distributions. We consider the class of distributions that correspond to

$$g(z) = (Az)^\alpha + Bz, \quad (2.17)$$

with  $A$  and  $B$  non-negative real numbers and  $\alpha$  given in (1.1). It is not difficult to verify that powers of  $z$ , less singular than  $z^\alpha$ , are irrelevant. For  $A > 0$ , probability distributions corresponding to (2.17) are stable distributions<sup>16</sup> with exponent  $\alpha$  which have been shifted by  $B$  along the real axis. For  $A = 0$ , (2.17) corresponds to a delta-function probability density concentrated at  $B$ . The constraint (2.16) gives

$$A^\alpha + B = 1. \quad (2.18)$$

Use of (2.15) and (2.17) yields

$$A'\lambda' = c^{1/\alpha}A \quad (2.19a)$$

and

$$B'\lambda' = a + cB, \quad (2.19b)$$

where  $A = A^{(n)}$  and  $A' = A^{(n+1)}$ , etc. The value of  $\lambda$  is fixed by (2.18). Using (2.18), a recursion relation may be written for  $A$  or  $B$  alone. For example,

$$(1-B')^{1/\alpha}/B' = c^{1/\alpha}(1-B)^{1/\alpha}/(a+cB). \quad (2.20)$$

From (2.19a) we see that, at a fixed point, either  $\lambda = c^{1/\alpha}$  or  $A = 0$ . We refer to the former case as the anomalous fixed point, and denote it by a subscript  $a$ . At

the anomalous fixed point

$$\lambda_a = c^{1/\alpha}, \quad (2.21a)$$

$$A_a = [(c^{1/\alpha} - c - a)/(c^{1/\alpha} - c)]^{1/\alpha}, \quad (2.21b)$$

and

$$B_a = a/(c^{1/\alpha} - c). \quad (2.21c)$$

The anomalous fixed point exists only if  $c^{1/\alpha} > c + a$  since we require that  $A$  be real and positive. The corresponding fixed-point distribution is a stable distribution which has been shifted by an amount  $B_a$ . Note that if the blobs had been treated as superconductors ( $a = 0$ ) as in Ref. 1, the fixed distribution would be an unshifted stable distribution ( $B = 0$ ).

We refer to the fixed point with  $A = 0$  as the ordinary fixed point and denote it with a subscript  $o$ . At the ordinary fixed point

$$\lambda_o = c + a, \quad (2.22a)$$

$$A_o = 0, \quad (2.22b)$$

and

$$B_o = 1. \quad (2.22c)$$

The ordinary fixed point is unstable to perturbations in  $A$  unless  $c^{1/\alpha} < c + a$ . Using (2.20) we have verified numerically that the anomalous fixed point is globally stable in the anomalous regime  $\lambda_a > \lambda_o$ , while the ordinary fixed point is globally stable in the ordinary regime  $\lambda_a < \lambda_o$ .

Let us now use the understanding we have gained of the scaling behavior of the distribution of chain resistances to study the scaling behavior of the conductivity. In the present model the backbone consists of a network of chains. The conductivity of this network is a homogeneous functional of the cumulative distribution of chain resistances  $F(R)$  and of the chain length,

$$\sigma[L, F(R)] = x^{d-2} y \sigma[xL, F(yR)]. \quad (2.23)$$

The RG analysis shows that  $F^{(n+1)}(\lambda R) = F^{(n)}(R)$  for large  $n$ , so that when  $x = b$  we require  $y = \lambda$  and the conductivity exponent is given by

$$t/\nu = (d-2) + \ln \lambda / \ln b. \quad (2.24)$$

Finally, using (2.7), (2.21a), (2.22a), and (2.24) we find

$$t = \begin{cases} t_o & \text{if } t_o > (d-2)\nu + 1/\alpha, \\ (d-2)\nu + 1/\alpha & \text{if } t_o < (d-2)\nu + 1/\alpha, \end{cases} \quad (2.25a)$$

$$(2.25b)$$

with  $t_o$  given in (2.7). This result agrees with Straley's.<sup>7</sup> In the anomalous regime the relation  $\ln \lambda / \ln b = 1/\nu\alpha$  does not depend on the values of the parameters  $a$ ,  $b$ , or  $c$ . Thus (2.25a) holds for the entire class of hierarchical models. Similarly, the crossover between the ordinary and anomalous regimes occurs when  $t_o = (d-2)\nu + 1/\alpha$ , independent of the model parameters. This observation lends support to the hypothesis that (2.25) is exact if  $t_o$  is interpreted as the true value of the conductivity exponent for ordinary percolation.

### III. NUMERICAL STUDY OF THE DISTRIBUTION OF CHAIN CONDUCTANCES

In this section we present the results of a numerical study of the probability distribution of chain conductances in order to confirm and clarify the analytic theory previously described. We have calculated the probability density  $P^{(n)}(W)$  of the conductance  $W^{(n)} = 1/R^{(n)}$  of an  $n$ -chain. The specific hierarchical model studied is shown in Fig. 1 and referred to in this section as the hierarchical model. For this model an  $(n+1)$ -blob is composed of two parallel  $n$ -chains so that  $a = \frac{1}{2}$  and an  $(n+1)$ -chain is composed of an  $(n+1)$ -blob in series with two  $n$ -chains so that  $c = 2$ . Thus the conductance of an  $(n+1)$ -chain is a random variable related to four independently chosen  $n$ -chain conductances,

$$\frac{1}{W^{(n+1)}} = \frac{1}{W_1^{(n)}} + \frac{1}{W_2^{(n)}} + \frac{1}{W_3^{(n)} + W_4^{(n)}}. \quad (3.1)$$

For comparison we have also studied the simpler case where  $(n+1)$ -chains are composed of four  $n$ -chains in series. This model, referred to as the series model, corresponds to  $a = 0$  and  $c = 4$ . Since there are no blobs in the series model, the results of Sec. II are exact. The series model corresponds to the chains in the nodes-links picture of the backbone.

For both models we choose the conductances of the elementary bonds from the probability density  $P^{(0)}(W)$ ,

$$P^{(0)}(W) = \begin{cases} \alpha W^{-(1-\alpha)}, & 0 < W \leq 1 \\ 0, & \text{otherwise.} \end{cases} \quad (3.2)$$

We studied five values of  $\alpha$ : 0.4, 0.5, 0.6, 0.66, and 0.9. For the hierarchical model the crossover between the ordinary and anomalous regimes occurs when  $\alpha = 0.757$ , so that  $\alpha = 0.9$  is in the ordinary regime and the four other values are in the anomalous regime. For the series model, all values of  $\alpha$  in the range  $0 < \alpha < 1$  are in the anomalous regime.

In a typical run,  $4^9$  bonds were chosen from the distribution (3.2) and  $4^8$  values  $W^{(1)}$  are calculated according to (3.1). A numerical approximation to  $P^{(1)}$  was obtained by putting these values of  $W^{(1)}$  into bins. The  $4^8$  values of  $W^{(1)}$  were then used to generate  $4^7$  values of  $W^{(2)}$  from which  $P^{(2)}$  was computed, etc. The corresponding calculation was also carried out for the series model. In Figs. 2 and 3 we show the probability densities obtained in this way for  $\alpha = 0.6$  and  $0.9$ , respectively. In these figures we plot  $P^{(n)}(W)$  versus  $\lambda^{(n)}W$  for  $n = 2$  (16384 values of  $W^{(2)}$ ), through  $n = 6$  (64 values of  $W^{(6)}$ ). The scaling factor  $\lambda$  is chosen according to (2.21a) or (2.22a). For the hierarchical model,  $\alpha = 0.6$  is in the anomalous regime and  $\lambda = 3.175$ , while  $\alpha = 0.9$  is in the ordinary regime where  $\lambda = 2.5$ . For the series model  $\lambda = 10.8$  for  $\alpha = 0.6$  and  $\lambda = 2.160$  for  $\alpha = 0.9$ .

Figures 2(a) and 2(b) show the evolution of the probability densities at  $\alpha = 0.6$  for the hierarchical and series models, respectively. It is clear from these figures that the predicted scaling leaves the small- $W$  tail of the distribution invariant from one generation to the next and that

the probability densities are approaching stable forms having the same power-law tail as the original distribution. The differences in the distribution between Figs. 2(a) and 2(b) appear only in the head ( $\lambda^n W \approx 1$ ) of the distribution, which cuts off more sharply for the hierarchical model than the series model. This supports Straley's<sup>7</sup> assertion that the nodes-links picture is adequate in the anomalous regime.

In Fig. 3 we show  $P^{(n)}(W)$  versus  $\lambda^n W$  for the hierarchical model with  $\alpha=0.9$  and  $\lambda=2.5$ , its theoretical value in the ordinary regime. This choice for  $\lambda$  leaves the location of the peak of the distribution nearly unchanged. As  $n$  increases, the head of the distribution becomes larger and more sharply peaked. The results are consistent with the theoretical prediction that the fixed-point density is a delta function.

For the special case  $\alpha=0.5$ ,  $P^{(n)}(W)$  can be compared directly to the theoretical predictions because there is a

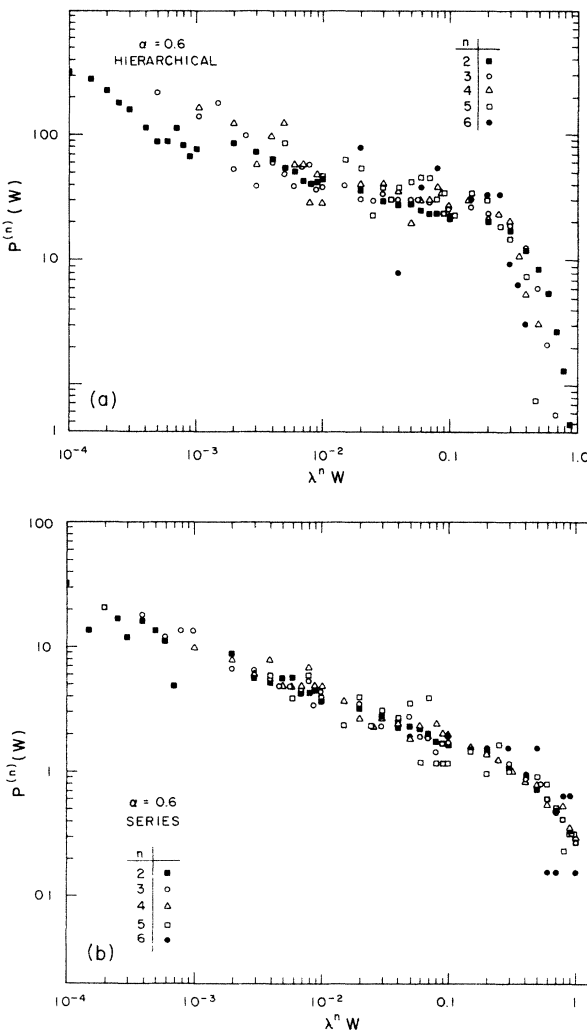


FIG. 2.  $P^{(n)}(W)$  vs  $\lambda^n W$  for  $\alpha=0.6$ . The probability density  $P^{(n)}(W)$  after  $n$  generations is plotted against the scaled conductance for  $2 \leq n \leq 6$ . (a) The hierarchical model and (b) the series model. The data represent 16384 values of  $W^{(2)}$  and 64 values of  $W^{(6)}$ .

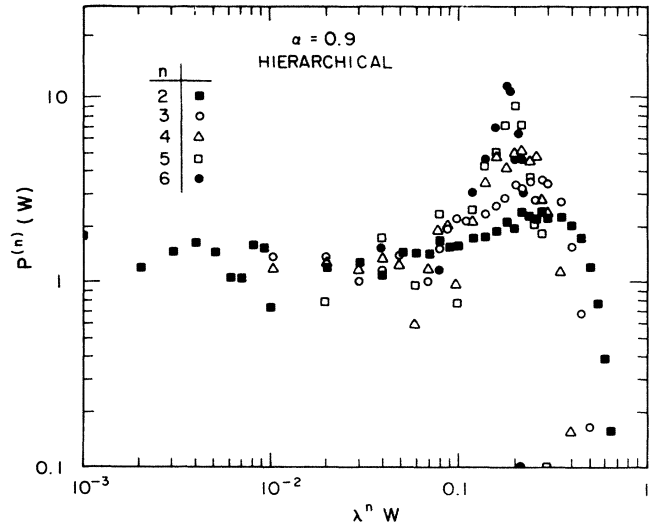


FIG. 3.  $P^{(n)}(W)$  vs  $\lambda^n W$  for  $\alpha=0.9$ . The probability density  $P^{(n)}(W)$  after  $n$  generations is plotted against the scaled conductance for  $2 \leq n \leq 6$  for the hierarchical model. The data represent 16384 values of  $W^{(2)}$  and 64 values of  $W^{(6)}$ .

closed-form expression for the probability densities,  $P(W | A, B)$ , corresponding to (2.17). The expression for  $P(W | A, B)$  is obtained from the known<sup>16</sup> expression for stable densities with exponent  $\frac{1}{2}$  by shifting through  $B$  and changing variables from  $R$  to  $W$ ,

$$P(W | A, B) = \begin{cases} (A/4\pi W)^{1/2} (1-BW)^{-1} \\ \times \exp[-AW/4(1-BW)], & 0 < W < B^{-1} \\ 0, & \text{otherwise.} \end{cases} \quad (3.3)$$

Since  $\alpha=0.5$  is in the anomalous regime,  $A$  is invariant under the renormalization-group transformation and, for the distribution (3.2), has the value  $\pi$ . For the hierarchical model at the anomalous fixed point, the ratio of  $A_a$  to  $B_a$  is determined by (2.21b) and (2.21c) and has the value  $9/4$ , so that for sufficiently large  $n$  we expect  $P^{(n)}(W)$  to approach to  $P(W | \pi, 4\pi/9)$ . For the series model,  $B_a=0$ , so we expect  $P^{(n)}(W)$  to approach  $P(W | \pi, 0)$  for large  $n$ .

Figures 4(a) and 4(b) show the results of a numerical study of  $P^{(n)}$  for  $\alpha=0.5$  with  $n=4$  and 5, respectively. Figure 4(a) shows  $P^{(4)}(W)$  and  $P^{(5)}(W)$  for the hierarchical model as compared to the theoretical fixed point,  $P(W | \pi, 4\pi/9)$ . Figure 4(b) shows the data for the series model for  $P^{(5)}(W)$  compared to the exact theoretical result for the fixed point,  $P(W | \pi, 0)$ . The similarity between  $P^{(4)}$  and  $P^{(5)}$  suggests that we are close to the fixed point by the fourth generation. For both the series and hierarchical models the agreement between the numerical and analytic probability densities is quite good. The influence of sample size in determining  $P(W)$  is seen in comparing in Fig. 4(a) with 15360 values of  $W^{(5)}$  and Fig. 4(b) with 256 values of  $W^{(5)}$ .

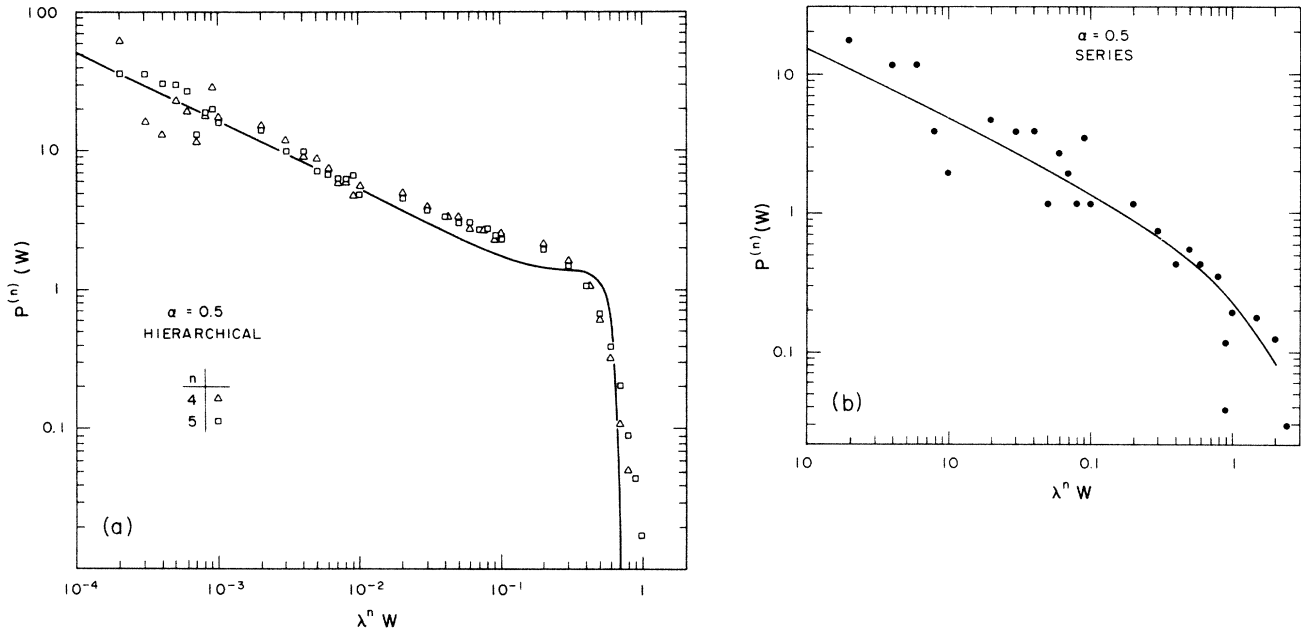


FIG. 4.  $P^{(n)}(W)$  vs  $\lambda^n W$  for  $\alpha=0.5$ . The probability density  $P^{(n)}(W)$  after  $n$  generations is plotted against the scaled conductance for  $n=4$  and 5. (a) The hierarchical model and (b) the series model. The data in (a) represent 61 440 values of  $W^{(4)}$  and 15 360 values of  $W^{(5)}$ . The data in (b) represent 1024 values of  $W^{(4)}$  and 256 values of  $W^{(5)}$ . The smooth curves in (a) and (b) are the predicted probability densities for the hierarchical and series models, respectively,  $P(W | \pi, 4\pi/9)$  and  $P(W | \pi, 0)$  as defined in (3.3).

In addition to studying the probability density we have also considered the average conductance  $W(S)$  at the  $n$ th generation as a function of the number of links,  $S$ , in that generation ( $S^{(n)}=c^n$ ). These results are shown in Figs. 5(a)–5(c), where  $W(S)$  is plotted against  $S$  for  $\alpha=0.9$ , 0.6, and 0.4, respectively. The data are obtained from four runs, each starting with  $4^9$  bonds with each data point corresponding to one generation. For large  $S$ ,  $\ln[W(S)]$  is a linear function of  $\ln S$  with a slope which is the conductivity exponent  $t$ . The solid lines in the figures show the theoretical slopes obtained from (2.5), (2.7), and (2.25). We note good agreement between the predicted slopes and the data.

Sen, Roberts, and Halperin<sup>8</sup> and Lubensky and Tremblay<sup>9</sup> have investigated the  $d=2$  percolation problem numerically using finite-size scaling. The largest lattice studied by Sen, Roberts, and Halperin was  $49 \times 49$  and the largest lattice studied by Lubensky and Tremblay was  $23 \times 23$ . For  $\alpha=0.4$ , Sen, Roberts, and Halperin obtain a result which is consistent with  $t=1/\alpha=2.5$ . However, for  $\alpha=0.66$  both Sen, Roberts, and Halperin and Lubensky and Tremblay obtain  $t=1.84$ , which is significantly above our theoretical prediction,  $t=1.5$ . Is this discrepancy a result of finite lattice sizes or a failure of the hierarchical model? To shed light on this question we calculated an effective exponent by taking the slope of lines connecting adjacent points on the graph of  $\ln[W(S)]$  versus  $\ln S$ . Figure 6 shows the slope found in this way as a function of the generation number  $n$  for  $\alpha=0.4$  and 0.66. For  $\alpha=0.4$  the effective slope oscillates around the theoretical prediction, while for  $\alpha=0.66$  the effective slope is larger than theoretical prediction and approaches it relatively slowly as  $n$  increases.

In order to make a quantitative comparison between the hierarchical model and an  $L \times L$  percolation lattice, it seems appropriate to choose  $n$  so that the number of links in the hierarchical lattice equals the average number of links in the backbone of the  $L \times L$  percolation lattice. Numerical simulations by Breton and Tremblay<sup>17</sup> show that the average number of links,  $S(L)$ , for the  $L \times L$  backbone is  $S(L) \approx (1.1)L^{3/4}$ . Comparing this to  $S=2^n$  for the hierarchical model, we find that  $n$  is between 3 and 4 for  $L=23$  and close to 4 for  $L=49$ . For  $n=4$  and  $\alpha=0.66$  the effective exponent in the hierarchical lattice is 1.75, which is significantly above the asymptotic prediction, 1.5. This finding is consistent with the hypothesis that simulations of Refs. 8 and 9 did not probe the scaling regime for  $\alpha=0.66$ .

#### IV. DISCUSSION AND CONCLUSIONS

Within the framework of a hierarchical model of the percolation backbone we have studied the effect of disorder in the bond strengths (conductances) of a percolation lattice. Our results support the view that there is a crossover in the conductivity exponent from the universal value to an anomalous value at the point where the two values are equal. The anomalous value is given by the simple expression  $t = [(d-2)\nu + 1/\alpha]$ . In the ordinary regime the conductivity of the percolation backbone depends on both the link and blob resistances and the conductivity exponent is therefore sensitive to the structural details of the blobs. On the other hand, in the anomalous regime the link resistances dominate the blob resistances; the conductivity near the threshold is determined only by the links leading to the simple expression for  $t$ .

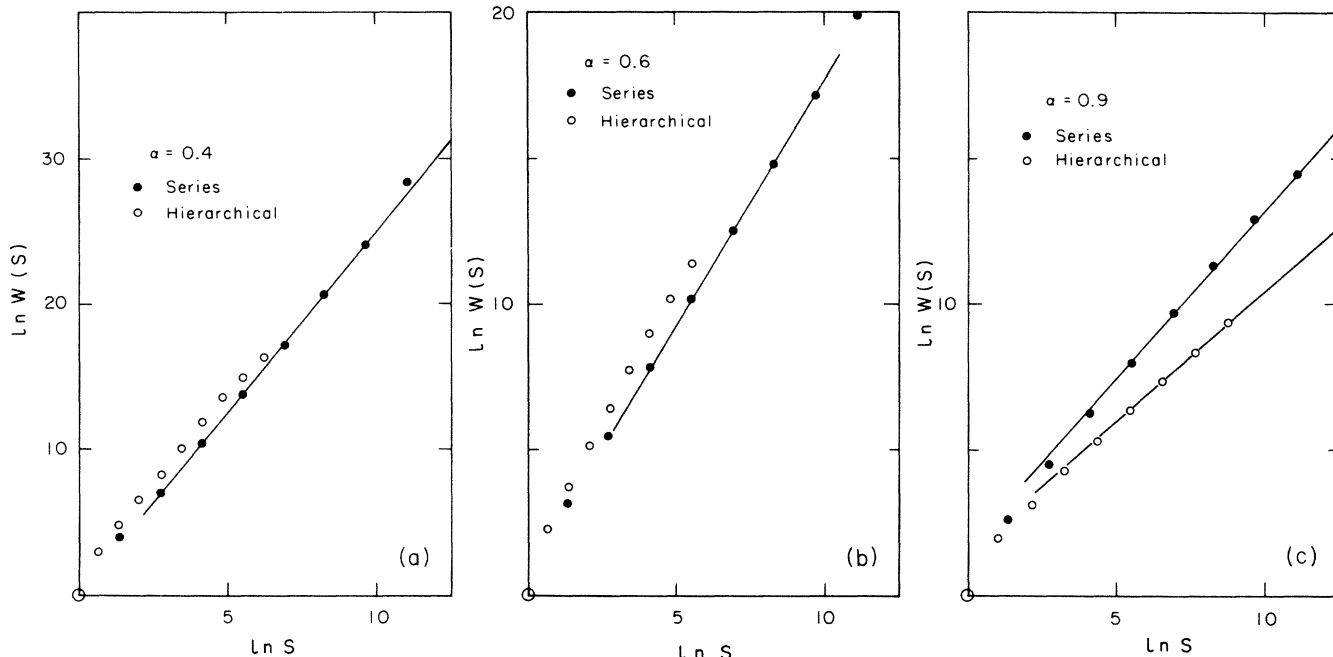


FIG. 5.  $\ln[W(S)]$  vs  $\ln S$ . The average conductivity is plotted against the number of singly-connected bonds for both the hierarchical and series models. (a)  $\alpha=0.4$ , (b)  $\alpha=0.6$ , and (c)  $\alpha=0.9$ . The solid lines are the theoretical slopes.

Lubensky and Tremblay<sup>9</sup> have studied the same problem using an  $\epsilon$  expansion. They predict that  $t$  is greater than the universal value whenever  $\alpha < 1$  and depends on both  $\alpha$  and  $\epsilon$  for  $\alpha$  near 1. They find a crossover to  $t = [(d - 2)\nu + 1/\alpha]$  at a value of  $\alpha$  which may be smaller than the crossover value found here. Their numerical simulations as well as those of Sen, Roberts, and Halperin<sup>8</sup> yield values of  $t$  which are larger than those predicted here and thus give qualitative support to the results of the  $\epsilon$  expansion. On the other hand, we showed that for the system sizes used in the simulations, the hierarchical model predicts an effective exponent which is larger than

the asymptotic exponent. Since both theories involve approximations and since both are consistent with the numerical results we cannot conclude at this time which is closer to the truth.

The hierarchical model incorporates many of the features of the nodes-links-blobs structure of the backbone and provides a simple framework for studying percolation problems. However, the hierarchical model does not include fluctuations in quantities such as the blob connectivity or the number of links between nodes and it is possible that these fluctuations might lead to a more complicated dependence of  $t$  on  $\alpha$  than found here. It would be very interesting to carry out more extensive simulations to determine whether the hierarchical model gives correct results for percolation with a broad distribution of bond strengths.

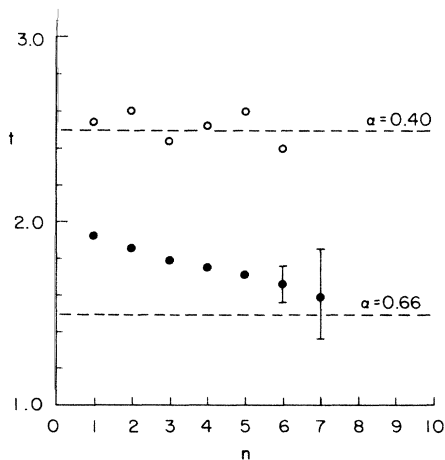


FIG. 6. Effective exponent as a function of generation number for  $\alpha=0.4$  and  $0.66$ . The effective exponent at generation  $n$  is the slope of the line connecting the  $n$ th and  $(n + 1)$ th data points in a plot of  $\ln[W(S)]$  vs  $\ln S$ .

ACKNOWLEDGMENTS

We are pleased to acknowledge André-Marie Tremblay for extensive and useful discussions. This work was supported in part by National Science Foundation Grants No. DMR-83-17442 and No. DMR-82-05352.

APPENDIX: PROPERTIES OF THE TYPICAL VALUE

The typical value  $r$  of a distribution  $F$  defined in (2.11), (2.12), and (2.14) exists for all distributions which are concentrated on the positive real axis. This follows from the facts<sup>16</sup> that the Laplace transform  $f(z)$  of any such distribution  $F$  exists for all real positive  $z$  with  $f(0)=1$ ,  $f(\infty)=0$ , and  $f(z)$  a monotone decreasing function. In particular, the typical value exists even if the mean value of the distribution fails to exist. For random variables re-

lated by a change of scale, the associated typical values are related by the same change of scale. That is, if cumulative distributions  $F_1$  and  $F_2$  are related by  $F_1(\lambda x) = F_2(x)$ , then their typical values are related  $r_1 = \lambda r_2$ .

If all of the moments of a distribution exist, then there is an implicit expression for  $r$  in terms of the cumulants  $\mathcal{K}_j$  of the distribution. Using the well-known cumulant expansion of the characteristic function, we have

$$\sum_{j=0}^{\infty} [(-1)^j \mathcal{K}_j / r^j j!] = 0, \quad (\text{A1})$$

where  $\mathcal{K}_0 \equiv 1$ . For a narrow distribution the mean  $\mathcal{K}_1$  is much greater than the standard deviation  $(\mathcal{K}_2)^{1/2}$ , which is, in turn, much greater than  $(\mathcal{K}_j)^{1/j}$  for  $j > 2$ , in which case (A1) can be inverted approximately to yield

$$r = \mathcal{K}_1 (1 - \mathcal{K}_2 / 2\mathcal{K}_1^2). \quad (\text{A2})$$

Thus we see that for narrow distributions, the typical value is close to and somewhat smaller than the mean value.

\*Present address: Department of Physics, Rensselaer Polytechnic Institute, Troy, NY 12181.

<sup>1</sup>B. I. Halperin, S. Feng, and P. N. Sen, *Phys. Rev. Lett.* **54**, 2391 (1985).

<sup>2</sup>A.-M.S. Tremblay, Shechao Feng, and P. Breton, *Phys. Rev. B* **33**, 2077 (1986).

<sup>3</sup>E. H. Hauge, in *Lecture Notes in Physics*, edited by G. Kirczenow and J. Marrow (Springer-Verlag, Berlin, 1974), Vol. 31.

<sup>4</sup>J. Machta and S. M. Moore, *Phys. Rev. A* **32**, 3164 (1985).

<sup>5</sup>P. M. Kogut and J. P. Straley, *J. Phys. C* **12**, 2151 (1979).

<sup>6</sup>A. Ben-Mizrahi and D. J. Bergman, *J. Phys. C* **14**, 909 (1981).

<sup>7</sup>J. P. Straley, *J. Phys. C* **15**, 2333 (1982); **15**, 2343 (1982).

<sup>8</sup>P. N. Sen, J. N. Roberts, and B. I. Halperin, *Phys. Rev. B* **32**, 3306 (1985).

<sup>9</sup>T. C. Lubensky and A.-M. S. Tremblay (unpublished).

<sup>10</sup>Our  $\alpha$  is defined as one minus the  $\alpha$  of Refs. 7 and 8.

<sup>11</sup>A. Skal and B. Shklovskii, *Fiz. Tekh. Poluprovodn.* **7**, 1589 (1973) [*Sov. Phys.—Semicond.* **8**, 1029 (1975)]; P. G. de Gennes, *J. Phys. (Paris) Lett.* **37**, L1 (1976).

<sup>12</sup>A. Coniglio, *J. Phys. A* **15**, 3829 (1982).

<sup>13</sup>H. E. Stanley, *J. Phys. A* **10**, L211 (1977); A. Coniglio, *Phys. Rev. Lett.* **46**, 250 (1981).

<sup>14</sup>L. de Arcangelis, S. Redner, and A. Coniglio, *Phys. Rev. B* **31**, 4725 (1985).

<sup>15</sup>H. J. Herrmann and H. E. Stanley, *Phys. Rev. Lett.* **53**, 1121 (1984).

<sup>16</sup>See W. Feller, *An Introduction to Probability Theory and its Applications*, 2nd ed. (Wiley, New York, 1971), Vol. 2, for a detailed discussion of the properties of Laplace transforms of distributions and the theory of stable distributions.

<sup>17</sup>A.-M. S. Tremblay (private communication).